Understanding the Distribution of Electric Currents in Active Regions and its Role for Eruptive Activity

A Step-2 Proposal to NASA:
Heliophysics Guest Investigator (H-GI)

Yang Liu (PI)
Stanford University

Philip H. Scherrer (Co-I)
Stanford University

Tibor Török (Co-I)
Predictive Science Inc.

James E. Leake (Co-I)
Naval Research Laboratory

Contents

1 Science Objectives and Significance (Intellectual Merit)

It is well established that solar flares and coronal mass ejections (CMEs) are powered by the free magnetic energy stored in volumetric electric currents in the corona, predominantly in active regions (ARs). However, it remains elusive how well these currents are neutralized, i.e., to what degree the main (or direct) coronal currents that connect the AR polarities are surrounded by shielding (or return) currents of opposite direction. This is an important question, since the current distribution of an AR may be closely related to its capability to produce eruptions. It has been argued, for example, that the presence of strong and concentrated return currents may impede or even inhibit the development of CMEs (Forbes 2010).

Despite its importance, the degree of current-neutralization in ARs has not yet been investigated systematically with state-of-the-art observations. Previous case studies, while far from being conclusive, indicate that the currents in isolated sunspots and simple, quiet ARs are well-neutralized, while significant non-neutralized (or net) currents exist in more complex, eruptive ARs (see § 2). This suggests a **so far unexplored relation between the degree of current-neutralization in ARs and their eruptive activity**. Such a relation, if found, **may open a new path for assessing the probability of ARs to produce eruptive flares and CMEs**, and therefore bears the potential for improving the forecasting of eruptions.

Clearly, systematic observational and numerical studies are needed to substantiate these preliminary results. We therefore propose a comprehensive observational investigation that will be supported by magnetohydrodynamic (MHD) simulations. Our goal is **to improve our understanding of the evolution and distribution of electric currents in ARs and to explore the possible relation between the degree of current neutralization and eruptive activity.** Specifically, we will address questions such as:

(i) What is the distribution of direct and return currents in ARs and does it differ significantly in quiet and eruptive regions? **(ii)** How well is the degree of current-neutralization in an AR correlated with magnetic shear along its main polarity inversion line (PIL) and its eruptive activity? **(iii)** How can the emergence of magnetically confined (thus, current-neutralized) sub-photospheric flux ropes lead to strongly non-neutralized AR currents in the corona? **(iv)** To what extent can return currents affect the onset of CMEs?

Our proposed effort is timely, relevant to NASA's goals (see § 5), and faces no technological barriers that would threaten its completion. As described below, our methodology provides a clear path toward achieving our goals, the data and numerical codes are available, and our team has the required experience.

2 Scientific Background and Motivation

Whether or not electric currents in ARs are neutralized is a long-standing question in solar physics. Before providing a brief overview of previous work on this topic, we note that current-neutralization must not be confused with "current-balance". Electric currents in magnetically well-isolated ARs have to be *balanced* to a very good approximation, as expected from $\nabla \cdot \mathbf{J} = 0$ (e.g., Georgoulis et al., 2012). What remains controversial is to which extent the currents are also *neutralized*, meaning that I calculated over a *single* AR polarity vanishes as well. Full neutralization requires the direct currents which connect the AR polarity centers to be surrounded by return currents of equal total strength and opposite direction (see Fig. 1(i)).

The notion that AR currents may be neutralized stems from the fact that isolated, current-carrying magnetic flux ropes, in which the field is confined to a certain radius, R, are current-neutralized. It has been argued by Parker (1996) that ARs are comprised of small, magnetically isolated flux ropes which are individually current-neutralized, so that a whole AR must be neutralized as well. Melrose (1991, 1995), however, argued that net (non-neutralized) currents can emerge from the solar interior with the emergence of magnetic flux. Longcope & Welsch (2000) devised a simplified model of flux-tube emergence that suggests that most of the return current is trapped below or at the photosphere, which supports Melrose's scenario.

Observationally, the distribution of direct and return currents can be inferred from photospheric vector

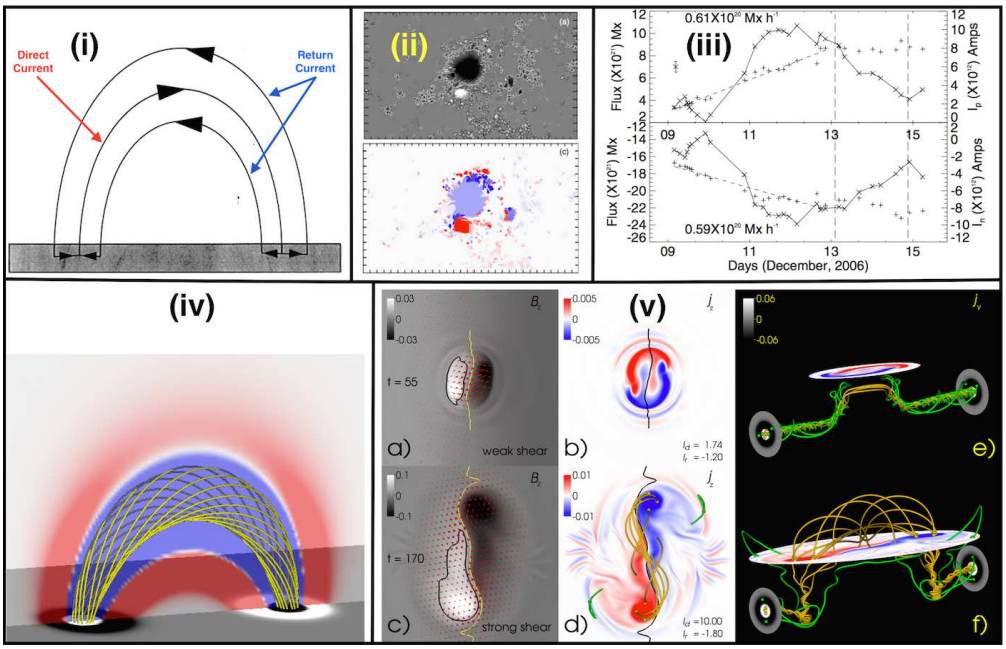

Figure 1: **(i)** Illustration of electric current distribution in an AR (adopted from Melrose, 1991). **(ii)** Hinode/SOT vertical magnetic field (top) and electric current density (bottom) of NOAA AR 10930 (from Georgoulis et al., 2012). **(iii)** Evolution of flux (+ symbols) and net vertical current ($\times$ symbols) in the northern (top) and southern (bottom) polarity of the same AR (from Ravindra et al., 2011). **(iv)** Model AR containing a flux rope produced by photospheric flows. The transparent plane shows direct (return) currents in blue (red). **(v)** Vertical magnetic field (left) and current density (center) at the photosphere in the flux emergence simulation by Leake et al. (2013), at an early (top) and evolved (bottom) state of emergence. The left panels also show the horizontal magnetic field (red arrows), outlining the development of strong shear along the PIL (yellow). The right panels show current density field lines at the same times. Direct currents are orange, return currents green. Most of the return currents remain trapped below the surface.

magnetograms by calculating the vertical current density, $J_z = \mu_0^{-1}(\frac{\partial By}{\partial x} - \frac{\partial Bx}{\partial y})$ (see § 3.1.2). Surprisingly, only few studies have been performed using observations. So far, data samples were considered only for isolated sunspots, which were found to be well-neutralized in most cases (Venkatakrishnan & Tiwari, 2009; Gosain et al., 2014). For ARs, the current distribution was obtained only for one quiet region (AR 10940; Georgoulis et al. 2012) and one highly-eruptive region (AR 10930; Ravindra et al. 2011; Georgoulis et al. 2012; Vemareddy et al. 2015). It was found that the currents in AR 10940 were well-neutralized, while strong net currents were present in AR 10930 (Fig. 1(ii-iii)). Furthermore, AR 10940 was characterized by relatively little shear along the PIL (the degree of alignment of the transverse magnetic field with the PIL direction), while the formation of AR 10930 was accompanied by substantial shear flows, leading to a strongly sheared PIL. We found the very same characteristics for the two ARs shown in Fig. 2 (quiet AR 11072 and eruptive AR 11158). Highly sheared PILs have been found to be closely related with eruptions (e.g., Schrijver, 2007). Thus, while being far from conclusive at present, these examples strongly suggest a relationship between the degree of current-neutralization, the amount of PIL shear, and eruptive activity of ARs. This relationship has not been explored so far, which is the main purpose of our investigation.

While our investigation will focus on analyzing and interpreting observational data, we will also employ MHD simulations. Our motivation for the latter is twofold: (i) simulations can be used to study physical aspects that cannot be easily addressed with present observations and (ii) the question of current-neutralization in ARs has so far been largely neglected in MHD simulations, with the few exceptions summarized below.

The observations described above suggest that eruptive ARs carry a strong net current. It is widely

accepted that such ARs are formed by the emergence of magnetic flux ropes from the solar interior into the corona (Leka et al., 1996). These ropes are believed to be magnetically well-isolated in the convection zone (Fan, 2009), i.e., to be current-neutralized to a very good approximation. This raises the important questions of (i) how neutralized sub-photospheric currents can transform into strong net coronal currents during flux emergence and (ii) which physical parameters determine the degree of current-neutralization in the resulting AR. Figure 1(v) shows that the flux-emergence simulation by Leake et al. (2013) (see § 3.2 for details) produces the characteristics of eruptive ARs relevant for this investigation (strong PIL shear and net current). Figure 2 additionally demonstrates its excellent agreement with the observations of AR 11158. Analyzing this simulation, Török et al. (2014) found that, as the rise of the flux rope temporarily halts before it breaches the photosphere, most of its return currents are pushed aside by the subjacent direct currents and remain trapped below the surface (Fig. 1(v)) – in line with the suggestions by Longcope & Welsch (2000).

However, as discussed in Török et al. (2014), the transformation from neutralized to non-neutralized currents appears to be far from trivial, since (i) the current paths become highly complex before and during the flux emergence, (ii) "short-circuiting" between current field lines may occur, (iii) only a fraction of the sub-photospheric currents enter the corona, and (iv) new currents may develop as a result of the shearing and converging flows associated with the emergence. Furthermore, only one parameter set of the model was analyzed in detail so far, so it remains to be understood which physical parameters are the most important ones for determining the degree of the final current-neutralization in the corona. We will use the model by Leake et al. (2013) to investigate these open questions (see § 4.2.1).

Another related, important question is to what extent return currents can affect the onset of eruptions. Theoretical considerations suggest that concentrated return currents surrounding a magnetic flux rope shield the direct current in the rope and so reduce the interaction of the rope with any other magnetic field (e.g., Forbes, 2010). This means that the presence of such return currents decreases the total Lorentz force within a coronal flux rope, which may suppress its eruption that otherwise would happen. This effect has not yet been studied in the context of solar physics, and we will attempt a first investigation in the proposed project.

Flux-emergence simulations are not well-suited for this task, since their coronal domains are typically too small to model full (i.e., CME-like) eruptions, and since it is not yet clear how the degree of current-neutralization can be "controlled" in these simulations. We will therefore use MHD simulations that are based on the second main mechanism for current-formation in ARs, namely the stressing of the coronal magnetic field by photospheric flows (e.g., Klimchuk & Sturrock, 1992). We will consider a model in which a current-carrying flux rope is produced by twisting a bipolar, potential magnetic field by localized vortex flows (see Fig. 1(iv) and § 3.2). Using such a model, Török & Kliem (2003) and very recently Dalmasse et al. (2015) showed that net currents develop if the flows are chosen such that they produce magnetic shear at the PIL, in line with the observations and the flux-emergence simulation mentioned above. The model allows one to control the degree of current-neutralization and to simulate full flux-rope eruptions, and is therefore perfectly suited for this task (§ 4.2.2).

Finally, we note that our investigation is also motivated by its relevance for theoretical models of solar eruptions. Many present CME simulations employ initial magnetic configurations that do not contain return currents (e.g., Török & Kliem, 2005; Manchester et al., 2008; Lugaz et al., 2011; Kliem et al., 2013) – and have therefore been criticized. While the observations and simulations mentioned above indicate a clear dominance of net current in eruptive ARs and, thus, support the use of such models, more observational and numerical investigations – as proposed in this effort – are required to substantiate such a modeling approach.

3 Methodology

With the availability of vector data from SDO/HMI, we now have for the first time the opportunity to investigate AR current-neutralization and its potential relation to eruptive activity with sufficiently large

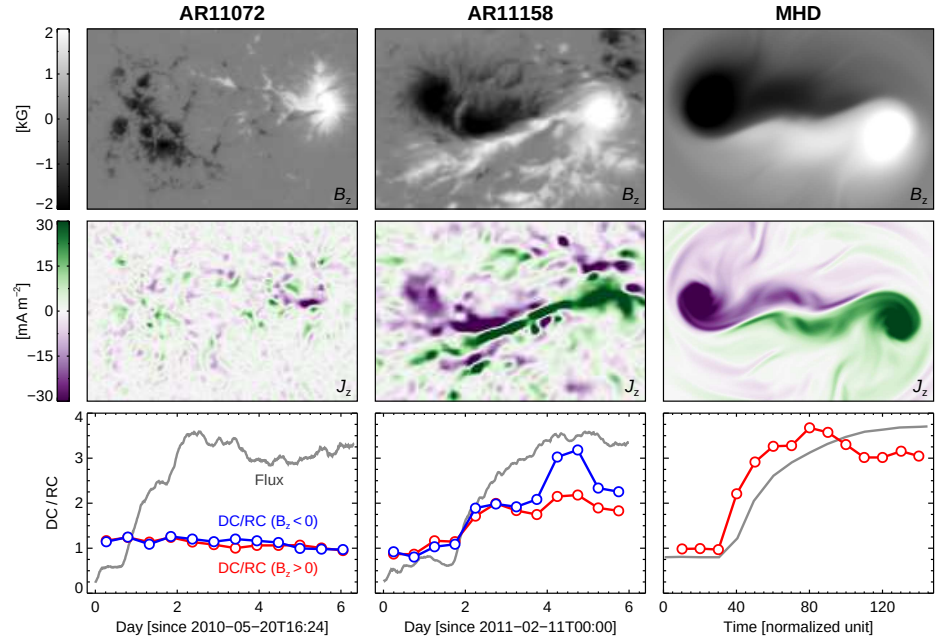

Figure 2: **Left**, **middle:** Vertical magnetic field and current density in quiet AR 11072 on 5 May 2010 and in the flare-productive center of AR 11158 on 15 Feb 2011. Bottom panels show the evolution of the unsigned magnetic flux (scaled to fit into the plot) and the direct/return current ratio, DC/RC. Red (blue) curves refer to the ratio obtained from $B_z > 0$ ($B_z < 0$) pixels. **Right:** Corresponding quantities for the MHD simulation by Leake et al. (2013). In the simulation, DC/RC is always the same for the two polarities, so only the ratio from $B_z > 0$ pixels is plotted here.

data samples. Furthermore, we can use MHD simulations to understand the underlying physics by studying aspects that cannot easily be addressed with observations. Before describing our technical approach in detail, we show as a demonstration in Fig. 2 photospheric maps of J_z and the ratio of the integrated direct and return current, DC/RC, for two ARs, together with a flux emergence simulation by Leake et al. (2013). AR 11072 is a simple bipolar region which does not exhibit strong magnetic shear along its PIL. The DC/RC ratio remains roughly close to one during the whole evolution of the AR, *i.e.*, the currents are almost perfectly neutralized. AR 11158, on the other hand, is complex with a quadrupole magnetic configuration. Only the inner polarity pair was relevant for the eruptive activity of the region and is therefore analyzed and shown in the figure. After the onset of significant flux emergence, the DC/RC ratio becomes significantly larger than one, i.e., the central part of the AR is strongly non-neutralized. The net currents are concentrated in the vicinity of the PIL, in very good agreement with the MHD simulation. AR 11158 was much more active than AR 11072, producing several major flares and CMEs during its disk passage. In comparison, AR 11072 did not produce any flares larger than C-class. These two cases strongly support the assumption that the degree of current-neutralization is related to the amount of PIL shear and to eruptive activity.

3.1 Observations

3.1.1 Data to be Used

Primary emphasis is on data from currently operating missions of the Heliophysics System Observatory (HSO). We will mainly use AR vector magnetic fields taken by SDO/HMI, together with SDO/AIA observations, GOES data, and online CME catalogs. The former will be used to measure current-neutralization and PIL shear, while the latter will be used to assess eruptive activity. Continuous observational coverage of HMI and AIA guarantees the collection of all ARs appearing on the Sun's disk without selection bias.

Figure 3: **Top**: Maps of B_z (*left*) and J_z (*right*) for AR 11158 with core-region mask (yellow and black contours, respectively) at 01:24 UT on 15 February 2011, shortly before the X2.2 flare. B_z is scaled to $\pm$ 1000 G; J_z is scaled to ± 44 mA cm^{-2}. Green (purple) colors show positive (negative) values of J_z. **Bottom**: Identification of the core region used for the DC/RC calculation. *Left:* Q-map at the lower boundary based on an NLFFF model. Dark lanes are high-Q contours. Pairs of star symbols indicate the magnetic-connectivity boundaries. Pink (green) stars are field-line foot points that close within the core region (connect to the outer AR polarities or to remote areas. *Right:* The yellow region shows the final mask, whereas the cyan areas shows pixels that were removed from the initially extracted region (see text for details). Selected field lines starting from pink and green stars are shown to illustrate the connectivities.

The HMI instrument provides full-disk photospheric vector magnetograms with 4096×4096 pixels. Its spatial resolution is about 1" with a 0.5" pixel size, at a cadence of 720 seconds. The vector data are de-projected to heliographic coordinates (Bobra et al., 2014). A detailed description of the HMI vector magnetic fields can be found in Hoeksema et al. (2014).

SDO/AIA provides continuous full-disk observations of the Sun in seven EUV and three UV-visible channels, with a cadence of up to 10 seconds and 1.5" resolution, sufficient to detect any large-scale activity. The GOES soft X-ray flux data can be obtained at, e.g., `http://www.swpc.noaa.gov/products/goes-x-ray-flux`. Several CME catalogs are available online, we will use mainly CDAW (`http://cdaw.gsfc.nasa.gov/CME_list/index.html`), SEEDS (`http://spaceweather.gmu.edu/seeds/secchi.php`), and CACTus (`http://sidc.oma.be/cactus/catalog.php`).

3.1.2 Calculation of Current-Neutralization

For each AR in our sample, the vertical electric current density, $J_z = \mu_0^{-1}(\frac{\partial By}{\partial x} - \frac{\partial Bx}{\partial y})$, will be derived from the processed SDO/HMI vector magnetic field data. In order to obtain the total direct and return current, positive and negative values of J_z will be integrated separately. The direct current, DC, is defined as the current that connects the polarity centers, which for each magnetic polarity of an AR determines the sign of J_z to be used for its integration. The return current, RC, is then the integral over the values of J_z of opposite sign for the same AR polarity. For each AR, the ratio of direct current and return current, DC/RC, will be computed for both AR polarities separately, as a function of time (see Fig. 2). That is, we will calculate the quantities $r^+ = DC(B_z > 0, t)/RC(B_z > 0, t)$ and $r^- = DC(B_z < 0, t)/RC(B_z < 0, t)$. For well-isolated, bipolar regions, we will select the area for the J_z integration "by eye", since for such regions most of the flux will connect from one polarity to the other. More complex ARs, however, will typically have significant flux that is not involved in the main eruptive activity of the AR, and therefore irrelevant

for our investigation. Such flux may connect either to other polarities of a multipolar region (as it was the case for AR 11158), to polarities of neighboring ARs, or to remote areas on the Sun. For such complex cases, we employ a combination of non-linear force-free field (NLFFF) extrapolations (Wiegelmann, 2004) and photospheric maps of the Squashing factor Q (Titov, 2007; Titov et al., 2011) to determine the relevant integration area (see below). ARs for which the signs of DC and RC or the relevant integration area cannot determined sufficiently well will be removed from the sample.

In order to illustrate the procedure for complex ARs, we present in Fig. 3 the vertical magnetic field and electric current density of the core region of AR 11158 at 01:24 UT on 15 February 2011. This core region produced an X2.2 flare about twenty minutes later. The complex AR had also two other large polarities to the East and the West of the core region (not shown in the figure), *i.e.*, there was substantial flux connecting the core region to the outer polarities. This flux played no role for the stability properties of the core flux that produced the eruption, so it needs to be excluded from our current-integration area. The yellow and black contours shown in the figure, the mask, encloses only the footpoints of closed field lines that connect the positive and negative polarity of the core field region, *i.e.*, the flux relevant for our investigation.

To obtain the mask, we first calculate Q at the lower boundary using an NLFFF model. The pattern of Q is complicated (Fig. 3; bottom left), but one can still identify an elongated patch encircled by high-Q contours. By tracing field lines along this contour, we see that it indeed outlines the boundary of closed flux connecting the core-field polarities (Fig. 3; bottom right). We then manually extract a region slightly larger than the area encircled by the high-Q contour and trace field lines from each pixel of the region; those with end points outside of the region are eliminated. Therefore all remaining field lines close within the region. To obtain the final mask (Fig. 3; bottom right), we apply two common morphology operators, dilation and erosion, to the input image, in order to remove noise, isolate individual elements, and join disparate elements. Figure 3 shows that the final mask covers most of the core polarities, but excludes significant flux, especially in the positive polarity. The DC/RC ratios obtained from the integration of the current densities within the masked area are $r^+ = 2.808 \pm 0.001$ and $r^- = 3.457 \pm 0.002$, respectively. The errors of the ratios are estimated from the errors of vector magnetic field data provided by SDO/HMI (Hoeksema et al., 2014). For comparison, the DC/RC ratios obtained from an area determined by "eye" (Fig. 2) are $r^+ = 1.916 \pm 0.001$ and $r^- = 2.394 \pm 0.001$. Obviously, DC/RC increases when irrelevant areas are excluded.

3.1.3 Calculation of PIL Shear

We will use the algorithm developed by Falconer et al. (2003, 2008) to determine the exact location of PILs. This algorithm has been successfully tested and used at Stanford University for MDI magnetograms (Mason & Hoeksema, 2010) and HMI vector magnetograms (Bobra et al., 2014), and is now available at Stanford's Joint Science Operations Center (JSOC). The amount of PIL magnetic shear will then be obtained by first calculating the angle between the PIL orientation and the horizontal magnetic field for a number of pixels along the PIL and then taking the average value. For example, for the core region of AR 11158 shown in Fig. 2, the averaged shear angle along the PIL is $13.6^o \pm 6.5^o$, while for AR 11072 we find $63.6^o \pm 23.8^o$. A smaller average shear angle thus corresponds to stronger magnetic shear.

3.1.4 Assessing Eruptive Activity

In order to establish a possible link between current-neutralization and eruptive activity, we have to monitor the latter for each AR we investigate. As a basic measure, we will use GOES data to assign to each AR a "flare-index" by summing the total number of flares (above C-class) during its disk passage, weighted by the flare magnitude. Since we are also interested in the question of whether return currents can suppress CMEs (§ 2), we will additionally use CME catalogs and AIA observations to assess each AR's CME-productivity, which we will then compare with the presence and strength of return currents in the AR.

3.2 Numerical Simulations

We will supplement our observational studies by MHD simulations, in order to address questions that cannot be efficiently addressed with present observations. We describe how we plan to employ the simulations in § 4. Here we restrict ourselves to a brief description of the numerical models we plan to use.

Flux-emergence model: The flux-emergence model we will use is described in detail in Leake et al. (2013). The MHD simulations presented in this work were performed by Co-I Leake, and analyzed with respect to electric current-neutralization in Török et al. (2014) by Co-I Török. The simulations model the dynamic emergence of a twisted sub-surface magnetic flux tube through the stratified layers of the Sun's convection zone, photosphere/chromosphere, transition region, and into the corona. These kinds of models have been successfully used for more than a decade to study various aspects of AR formation (e.g., Fan, 2001; Manchester et al., 2004; Archontis & Török, 2008). In addition the simulations of Leake et al. (2013) included the interaction of the emerging magnetic flux with a pre-existing, arcade-like coronal magnetic field. Figures 1(v) and 2 show snapshots of one of the simulations.

In these dynamics simulations, the initial sub-surface flux rope is current-neutralized, as it is located in a region of high plasma-β and thus the magnetic field is localized. The initial flux rope is made buoyant for part of its section, creating a rising Ω-shaped loop which reaches the model surface. The halt of the rope's rise is caused by the stable photosphere and atmosphere above, which causes a flux pile-up near the surface, and large horizontal expansion, until a period of time when the piled-up magnetic flux can penetrate the surface and emerge into the corona, interacting with the pre-existing coronal field. As in the analytical model of Longcope & Welsch (2000), initially the emerging field has very little twist compared to the original twist in the flux rope, and this leads to the propagation of twist into the corona, along with strong shearing motions near the PIL, driven by the Lorentz force in the expanding field region. It is these flows that are likely the source of the redistribution of the electric currents, which results in the emerging field being non-neutralized. I.e., the emergence process results in a volumetric net current in the corona, with the return currents confined to the surface (Fig. 1(v)). More careful analysis of the simulations is required to understand exactly how this process operates on the Sun (see § 4.2.1)

The analysis in Török et al. (2014) was performed for only one realization of the parameter space of the flux-emergence model. The free parameters of the model which are expected to affect the amount of shearing and non-neutralization of electric currents, to presumably various degrees, are the size, strength, geometry, twist, and buoyancy of the initial magnetic flux rope in the convection zone, as well as the configuration and strength of the pre-existing coronal magnetic field. We describe in § 4.2.1 how we plan to employ the model for the purpose of our investigation.

Photospheric-Flow Model: The stressing of the coronal magnetic field by photospheric flows is the second main mechanism by which electric currents may develop in ARs. The formation of arched, current-carrying coronal flux ropes by such flows has been extensively studied using MHD simulations (e.g., Amari et al., 1996; Török & Kliem, 2003; Aulanier et al., 2005; Dalmasse et al., 2015). In all of these models a bipolar potential field (Fig. 4b) is slowly twisted by sub-alfvénic vortex flows, imposed around the two polarity centers at the photosphere (Fig. 4a). This produces a flux rope anchored in the two polarities, and successively increases its current until the rope may loose equilibrium and erupts (Fig. 4c). If the twisting is stopped before that point, stable flux-rope equilibria –reminiscent of a bipolar AR– are obtained.

For our investigation we will employ the photospheric-flow model by Török & Kliem (2003), which has been used predominantly to study the formation of coronal flux ropes and the onset conditions for their eruption. The simulations are performed in a Cartesian domain that is sufficiently large to model full (CME-like) eruptions. The vortex flows are imposed along the contours of $B_z(z = 0)$, so that the initial "magnetogram" is preserved throughout the simulation. A variety of initial magnetic fields can be used, and the width and velocities of the vortex flows can be freely varied. The degree of current-neutralization can be adjusted by choosing appropriate initial fields and flow profiles (see § 4.2.2).

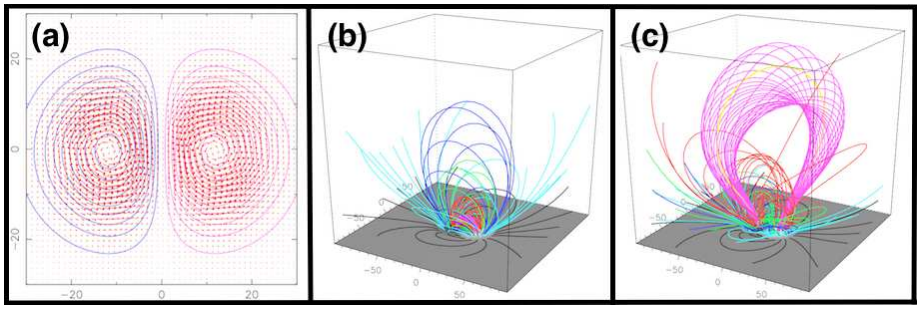

Figure 4: Photospheric-flow MHD simulation (adopted from Aulanier et al., 2005). **(a)** Vortex flows (arrows) and B_z contours at photospheric boundary. **(b)** Initial potential field. **(c)** Flux-rope eruption after sufficient twisting has been applied.

4 Proposed Work

4.1 Relationship between Current-Neutralization, PIL Shear, and Eruptive Activity

As outlined in the first two sections, the main task of our proposed investigation is to use observations to search for a relationship between the degree of current-neutralization, the amount of magnetic shear at the PIL, and the eruptive activity of ARs. As further described in § 3.1.1, we have so far collected 428 ARs and expect to extend this data set by about 120 new ARs by the beginning of this investigation.

We will examine the extent of validity of a relationship between these quantities using this large data sample. For each AR, we will calculate the degree of current-neutralization from two conjugate patches of opposite polarity surrounding PILs (the DC/RC ratio; see § 3.1.2) and the magnetic shear along those PILs (§ 3.1.3), during the observable evolution of the AR. We will also identify and catalog all significant eruptions during this evolution (§ 3.1.4). For ARs that are not associated with any eruptions, we will average DC/RC and the PIL shear over the time period starting when DC/RC reaches saturation (which is, for example, on May 20 for the AR 11072 shown in Fig. 2) to obtain for each AR a representative, single number of the relevant quantities. For ARs that are associated with eruptions, we will average DC/RC and the shear along the eruption-producing PILs (average over half hour to one hour to decrease the noise) before each event to obtain for the AR the relevant quantities for this event. We will then finally uses the thus obtained representative values to search for correlations between our quantities.

Apart from this general statistical study, we will also select a number of well-observed cases of both quiet and eruptive ARs (such as the examples shown in Fig. 2) for more detailed examination and direct comparison with the MHD simulations. These case studies will include, for example, investigations of (i) the details of the development of current-neutralization and PIL shear in the early phase of flux emergence, (ii) the morphology (distribution) of the direct and return currents, and (iii) the possible existence of a critical value of DC/RC or net current that could be used as a threshold for the onset of eruptions.

4.2 Tasks Using Numerical Simulations

4.2.1 Investigating Current Formation in ARs by Flux Emergence

The study of Török et al. (2014), using one of the simulations by Leake et al. (2013), suggests that the dynamic emergence of a twisted magnetic flux tube results in a strongly non-neutralized coronal current configuration, during the formation of a highly-sheared AR (see Figs. 1 and 2). We propose to both continue to study the simulations of Leake et al. (2013), and to perform a parametric study, varying free parameters of the model, to further understand the origin of non-neutralization of coronal electric currents in ARs.

By studying the connectivity of electric currents, we can track the evolution of the direct and return currents through time in the existing simulations. Combining this with a study of the current-density flux, we will obtain a more complete theoretical understanding of how a sub-surface, current-neutralized flux rope can emerge to become a non-neutralized AR. Unlike magnetic flux, ideal motions can lead to the generation

and destruction of current density flux. The region where the buoyant rise of the convection zone flux rope is halted by the stable surface layers before it can emerge into the corona, and the subsequent deformation of the flux rope, is a likely source of ideal flows which can create and destroy direct and return currents.

The initial parameters of the simulations, such as the amount of magnetic flux and twist in the convection-zone flux rope, its size and depth, and its orientation with respect to the pre-existing coronal field, are all likely to produce varying degrees of AR shearing and ultimately net current. We are in an advantageous situation of being able to use these simulations to create relationships between AR shear, twist, and electric current-neutralization. We will perform multiple simulations, varying these parameters, and calculate the amount of shear along the PIL, twist, and net current. Initial simulations suggest that the relationship between these quantities is not simple, which necessitates the use of these MHD simulations.

The simulations by Leake et al. (2013) model relatively small ARs with a spatial extension of about 15–20 Mm. While there is no obvious reason to expect that the formation and final distribution of electric currents depends strongly on the AR size, we will also perform simulations with larger AR extensions ($\lesssim 50$ Mm) and magnetic flux ($\lesssim 10^{22}$ Mx) to ensure that the underlying mechanisms also operate on these more realistic AR scales.

4.2.2 Investigating the Effect of Return Currents on the Onset of Eruptions

We will use MHD simulations of the photospheric-flow model by Török & Kliem (2003) (§ 3.2) to investigate to what extent the presence of return currents can effect the onset of eruptions (specifically CMEs) in ARs. The model allows to obtain an essentially arbitrary degree of current-neutralization by adjusting the distance of the photospheric polarities of the initial potential field and the width of the vortex flows. As long as both are chosen such that no shear develops along the PIL, the system remains fully neutralized. As the distance of the polarities is decreased and/or the width of the vortices is increased, stable flux-rope configurations with increasing shear and net current can be produced. Furthermore, adjusting the flow profiles by letting the velocities decrease differently with distance from the polarity centers or by changing the flow direction at a certain distance allows one to adjust the width (i.e., the compactness) of the return currents.

We will employ these properties to perform a parametric study in which we will vary the degree of current-neutralization and the compactness of the return currents for a given amount of direct current in the flux rope. We will, for different initial magnetic fields, first produce a configuration with no or little return current and determine the amount of direct current (or flux-rope twist) required to produce an eruption. We will then systematically increase the strength of both direct and return currents, as well as the compactness of the latter, and test under which conditions stable configurations with stronger direct currents can be obtained. The simulations will be performed in the $\beta = 0$ approximation, which is computationally efficient and physically justified (since coronal eruptions are driven mainly by the Lorentz force).

While our focus will be primarily on understanding the effects of return currents on the onset conditions of eruptions, we will also quantify for all our simulations the DC/RC ratio and the PIL shear, and we will compare them with the results of the flux-emergence simulations and our observational investigation.

4.3 Data and Model Readiness

We will predominantly use SDO/HMI magnetograms and derived data products routinely produced at SDO JSOC (Stanford University). The latter include the algorithm for identifying PILs (Bobra et al., 2014), the module for NLFFF extrapolations (Sun et al., 2012), and Q-maps.[1] Data and data products are and will be made available to the community through the JSOC website (`http://jsoc.stanford.edu`). The CME catalogs and the GOES and AIA data required to identify eruptive activity for each AR are publicly

[1] Q-maps will be produced under our NASA grant "Q-Maps: A New Synoptic Data Product for Investigating Dynamic Coronal Connectivity"; PI: Dr. J. T. Hoeksema, by ROSES 2014 HGI ODDE.

available. We have been collecting a sample of 428 ARs for the time period 05/2010 to 01/2016, including 166 emerging ARs. We expect to extend our dataset by about 120 new ARs by the start of this investigation. This will provide us with a sample of about 528 ARs, sufficiently large for a statistical investigation.

The flux-emergence simulations (§ 3.2) will be performed with the *Lare3D* MHD code (Arber et al., 2001), which uses a Lagrangian-Remap implementation on a staggered, Cartesian grid, which ensures non-divergence of the magnetic field. The code has been used to study flux emergence and coronal dynamics for over 10 years. It is highly parallelized using the *Message Passing Interface* (MPI), and scales to a few thousand cores. Typical runs, utilizing stretched grids of size $\sim 300^3$, take about 96 hours on 512 cores of a high performance computer (HPC) totaling $\approx$ 50,000 cpu-hours. Co-I Dr. Leake has access to $\approx$ 5 million cpu-hours, a significant portion of which will be allocated to the proposed work. HPC time is provided by the Department of Defense's *High Performance Computing Modernization Program* (HPCMP).

The MHD code for the simulations of AR formation by photospheric flows (§ 3.2) was developed by Co-I Dr. Török and Dr. B. Kliem (Török & Kliem, 2003). It has been used for 16 years for the modeling of various aspects of solar eruptive activity. The simulations proposed here will be performed in the $\beta = 0$ approximation, require no parallelization, and can therefore be run on standard PCs or workstations. Sufficient computing power for the completion of the proposed runs is available at Predictive Science Inc.

5 Relevance to NASA's Heliophysics Program and Broader Impacts

The proposed work will investigate the link between current-neutralization, PIL shear, and eruptive activity in solar ARs, which bears the potential of opening a new path for the forecasting of solar eruptions.

The proposal is responsive to ROSES – 2016 B.4. "Heliophysics Guest Investigators (H – GI/Open)" in the Open program with primary emphasis on "the analysis of data from currently operating missions of the Heliophysics System Observatory (HSO)." It meets the program goal "to maximize the scientific return from operating Heliophysics missions" and is highly relevant to the Heliophysics Decadal Survey Key Science Goal #1: "Determine the origins of the Sun's activity and predict the variations in the space environment." It is also relevant to the goals of the SDO mission "What magnetic field configurations lead to the CMEs, filament eruptions, and flares that produce energetic particles and radiation?" and "When will activity occur, and is it possible to make accurate and reliable forecasts of space weather and climate?"

6 Work Plan, Management, and Personnel Commitments

Year 1: For a sample of about 270 ARs, process HMI vector data and analyze current distribution, PIL shear, and eruptive activity. Model AR formation by photospheric flows with varying degree of current-neutralization and analyze the current-evolution in existing flux-emergence simulations. **Year 2:** Observational analysis same as for year 1, now for a sample of about another 270 ARs. Combine results with the sample obtained in year 1 and carry out statistical analysis. Continue simulations of AR formation by photospheric flows and perform flux-emergence simulations with different amounts of sub-photospheric flux-rope twist. **Year 3:** Finalize simulation series and compare them to the observational results.

PI Dr. Y. Liu will have the overall responsibility for the project. He will coordinate all research efforts of the team, collect new ARs, evaluate and process observational data, and use the results to suggest simulation parameters. Co-I Dr. J. E. Leake will perform the *Lare3D* simulations and study how electric currents reorganize during flux emergence. Co-I Dr. T. Török will design and run the simulations of AR formation by photospheric flows and assist Dr. Leake in designing and analyzing the flux-emergence simulations. He will also assist the PI in interpreting the observations. Co-I Dr. P. H. Scherrer will be available for discussions and provide scientific insight, particularly in assisting the PI in the interpretation of the HMI data.

References

Amari, T., Luciani, J. F., Aly, J. J., & Tagger, M. 1996, ApJ, 466, L39

Arber, T. D., Longbottom, A. W., Gerrard, C. L., & Milne, A. M. 2001, Journal of Computational Physics, 171, 151

Archontis, V., & Török, T. 2008, A&A, 492, L35

Aulanier, G., Démoulin, P., & Grappin, R. 2005, A&A, 430, 1067

Bobra, M. G., Sun, X., Hoeksema, J. T., Turmon, M., Liu, Y., Hayashi, K., Barnes, G., & Leka, K. D. 2014, Sol. Phys., 289, 3549

Dalmasse, K., Aulanier, G., Démoulin, P., Kliem, B., Török, T., & Pariat, E. 2015, ApJ, 810, 17

Falconer, D. A., Moore, R. L., & Gary, G. A. 2003, J. Geophys. Res., 108, 1380

—. 2008, ApJ, 689, 1433

Fan, Y. 2001, ApJ, 554, L111

—. 2009, Living Reviews in Solar Physics, 6, 4

Forbes, T. 2010, in Heliophysics: Space Storms and Radiation: Causes and Effects, ed. C. J. Schrijver & G. L. Siscoe (Cambridge (UK): Cambridge University Press), 159

Georgoulis, M. K., Titov, V. S., & Mikić, Z. 2012, ApJ, 761, 61

Gosain, S., Démoulin, P., & López Fuentes, M. 2014, ApJ, 793, 15

Hoeksema, J. T., et al. 2014, Sol. Phys., 289, 3483

Kliem, B., Su, Y. N., van Ballegooijen, A. A., & DeLuca, E. E. 2013, ApJ, 779, 129

Klimchuk, J. A., & Sturrock, P. A. 1992, ApJ, 385, 344

Leake, J. E., Linton, M. G., & Török, T. 2013, ApJ, 778, 99

Leka, K. D., Canfield, R. C., McClymont, A. N., & van Driel-Gesztelyi, L. 1996, ApJ, 462, 547

Longcope, D. W., & Welsch, B. T. 2000, ApJ, 545, 1089

Lugaz, N., Downs, C., Shibata, K., Roussev, I. I., Asai, A., & Gombosi, T. I. 2011, ApJ, 738, 127

Manchester, IV, W., Gombosi, T., DeZeeuw, D., & Fan, Y. 2004, ApJ, 610, 588

Manchester, IV, W. B., et al. 2008, ApJ, 684, 1448

Mason, J. P., & Hoeksema, J. T. 2010, ApJ, 723, 634

Melrose, D. B. 1991, Astrophys. J., 381, 306

—. 1995, Astrophys. J., 451, 391

Parker, E. N. 1996, Astrophys. J., 471, 485

Ravindra, B., Venkatakrishnan, P., Tiwari, S. K., & Bhattacharyya, R. 2011, ApJ, 740, 19

Schrijver, C. J. 2007, ApJ, 655, L117

Sun, X., Hoeksema, J. T., Liu, Y., Wiegelmann, T., Hayashi, K., Chen, Q., & Thalmann, J. 2012, Astrophys. J., 748, 77

Titov, V. S. 2007, Astrophys. J., 660, 863

Titov, V. S., Mikic, Z., Linker, J. A., Lionello, R., & Antiochos, S. K. 2011, Astrophys. J., 731, 111

Török, T., & Kliem, B. 2003, A&A, 406, 1043

—. 2005, ApJ, 630, L97

Török, T., et al. 2014, ApJ, 782, L10

Vemareddy, P., Venkatakrishnan, P., & Karthikreddy, S. 2015, Research in Astronomy and Astrophysics, 15, 1547

Venkatakrishnan, P., & Tiwari, S. K. 2009, ApJ, 706, L114

Wiegelmann, T. 2004, Sol. Phys., 219, 87